Ecological Indicators 64 (2016) 281–288

Contents lists available at ScienceDirect

Ecological Indicators

journal homepage: www.elsevier.com/locate/ecolind

Land surface phenology as an indicator of biodiversity patterns

Andrés Viña [a,*], Wei Liu [a,1], Shiqiang Zhou [b], Jinyan Huang [b], Jianguo Liu [a]

[a] Center for Systems Integration and Sustainability, Department of Fisheries and Wildlife, Michigan State University, East Lansing, MI, USA
[b] China Conservation and Research Center for the Giant Panda, Wolong Nature Reserve, Wenchuan, Sichuan, China

ARTICLE INFO

Article history:
Received 31 August 2015
Received in revised form
25 November 2015
Accepted 6 January 2016

Keywords:
Biodiversity
Floristic similarity
Image fusion
Landsat
MODIS
Phenologic similarity
Spectral vegetation indices
Visible atmospherically resistant index

ABSTRACT

With the rapid decline in biodiversity worldwide it is imperative to develop procedures for assessing changes in biodiversity across space. The synoptic view provided by imaging remote sensors constitutes a suitable approach for analyzing biodiversity from local to regional scales. A procedure based on the close relationship between floristic similarity and the similarity in land surface phenology was recently developed and successfully applied to assess diversity patterns using time series imagery acquired by the Moderate Resolution Imaging Spectro-radiometer (MODIS). However, as it depends on high temporal resolution remotely sensed data (e.g., MODIS), the procedure is constrained by the coarse spatial resolution characterizing these high temporal resolution data. Using an optimized technique for image fusion, we combined high temporal resolution data acquired by the MODIS sensor system with moderate spatial resolution data acquired by the Landsat TM/ETM+ sensor systems. Our results show that the MODIS/Landsat data fusion allows the characterization of land surface phenology at higher spatial resolutions, which better corresponded with information acquired within vegetation survey plots established in temperate montane forests located in Wolong Nature Reserve, Sichuan Province, China. As such, the procedure is useful for capturing changes in biodiversity induced by disturbances operating at large spatial scales and constitutes a suitable tool for monitoring and managing biodiversity.

© 2016 Elsevier Ltd. All rights reserved.

1. Introduction

Human activities continue to put pressure on biodiversity around the globe. To develop effective conservation actions it is imperative to analyze and monitor the spatio-temporal dynamics of biodiversity (such as the number and composition of species), particularly in response to human-induced disturbances. Such analyses require indicators that allow fast, synoptic and accurate assessments of biodiversity patterns at multiple scales (Turner, 2014). The synoptic view provided by imaging remote sensors constitutes a suitable approach for analyzing biodiversity from local to regional scales (Rose et al., 2015; Turner, 2014; Turner et al., 2003). Some studies have evaluated direct pixel-based relationships between the spatial patterns of biodiversity and multispectral imagery (Rocchini, 2007; Rocchini et al., 2010; Thessler et al., 2005; Tuomisto et al., 2003), while others utilize extensive spectral libraries of individual plant species that are then used to map biodiversity patterns using hyper-spectral imagery (Asner and Martin, 2008, 2009; Carlson et al., 2007; Féret and Asner, 2014). Yet, these methods have not seen a widespread adoption due to the low availability and high economic cost of pertinent remotely sensed data (e.g., hyper-spectral imagery). In addition, these methods tend to be constrained to particular geographic locations, individual species and/or species assemblages, and do not necessarily account for the seasonal variability of canopy spectral characteristics in response to the phenologic dynamics of vegetation.

Alternatively, novel procedures for remotely assessing the spatial and temporal changes in the distribution of individual species and of regional biodiversity pools have been devised based on the use of data acquired with a high temporal resolution (Tuanmu et al., 2010; Viña et al., 2008, 2012). Specifically, these procedures have been used for evaluating the spatial distribution of understory species (Tuanmu et al., 2010), for analyzing wildlife habitat suitability (Liu and Viña, 2014; Tuanmu et al., 2011; Viña et al., 2008, 2010), and for evaluating floristic similarity patterns across space (Viña et al., 2012). Based on the close relationship between floristic similarity and the similarity in land surface phenology, these procedures are suitable for assessing the effectiveness of conservation activities (Viña et al., 2012). Their drawback is that the high temporal resolution remotely sensed data required for them are

* Corresponding author at: Center for Systems Integration and Sustainability, 1405 S. Harrison Road, Suite 115 Manly Miles Bldg., Michigan State University, East Lansing, MI 48823-5243, USA. Tel.: +1 517 798 6712.
E-mail address: vina@msu.edu (A. Viña).
[1] Present address: International Institute for Applied Systems Analysis, Laxemburg, Austria.

http://dx.doi.org/10.1016/j.ecolind.2016.01.007
1470-160X/© 2016 Elsevier Ltd. All rights reserved.

also acquired at coarse spatial resolutions (ca. 250 × 250 m/pixel or larger), which in most cases do not completely relate with the spatial resolution of the field data used to calibrate them. The main goal of this study was to explore the suitability of using land surface phenology obtained through the fusion of high temporal resolution but coarse spatial resolution data (i.e., MODIS) with moderate spatial resolution data (i.e., Landsat TM/ETM+) as an indicator of floristic similarity patterns across space.

2. Methods

2.1. Study region

The Wolong Nature Reserve was established in 1975 and currently encompasses ca. 200,000 ha (Liu et al., 1999) (Fig. 1). It is one of the largest nature reserves designated for the conservation of the endangered giant panda (*Ailuropoda melanoleuca*) and contains ca. 10% of the entire wild panda population (State Forestry Administration, 2006). Situated between the Sichuan Basin and the Qinghai-Tibet Plateau in China's southwest Sichuan province, it is characterized by a strong elevational range, from ca. 1200 m to more than 6200 m. Mean annual rainfall is ca. 880 mm, with the monsoon between June and September typically bringing a high frequency of heavy rainfall events (Schaller et al., 1985). Due to its large elevational range, rugged terrain and complex geology and soils, the Reserve exhibits high biological diversity, containing more than 6000 species of plants and animals. In fact, it is located within one of the top global biodiversity hotspots, the Southwest China biodiversity hotspot (Liu et al., 2003; Myers et al., 2000). Vegetation is dominated by temperate montane forests which by 2007 comprised about 38% of the Reserve (Viña et al., 2011), with evergreen and deciduous broadleaf stands located at lower elevations and subalpine coniferous stands located at higher elevations. The dense understory of these forests is dominated by bamboo species such as *Bashania fabri* and *Fargesia robusta*, the staple food of the giant panda (Reid and Hu, 1991; Schaller et al., 1985; Taylor and Qin, 1993).

The Reserve is also home to more than 5000 local residents in over 1200 households distributed in six villages (Fig. 1). These local residents are mainly dependent on farming. In recent years the Reserve has experienced a boom in tourism, with a 10-fold increase in the number of visitors, from ca. 20,000 in the 1990s (Lindberg et al., 2003) to more than 200,000 in 2006 (He et al., 2008). This

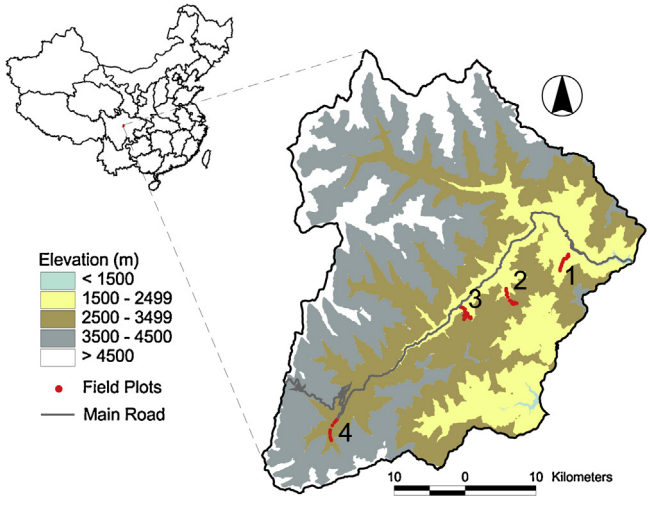

Fig. 1. Topographic map of the study region (i.e., Wolong Nature Reserve) showing the locations of the main road and of the 62 field plots (red dots; not scaled) established along four trails (numbered).

increase has been accompanied by rapid development of tourism infrastructure (e.g., hotels, restaurants), together with road construction. Previous studies have shown that many forest areas have been replaced by other land cover types resulting in rapid degradation of forests and panda habitat, so that from 1974 to 1997 the degradation continued unabated, and the fragmentation of high-quality panda habitat became more severe (Liu et al., 2001; Viña et al., 2007). More recently, however, the deforestation trend inside the Reserve has been slowing due in part to the implementation of national conservation policies (Viña et al., 2007, 2011).

Due to its highly dynamic natural and human components and their interrelations, this Reserve is an ideal coupled human and natural system for examining the dynamics of biodiversity. Our research group has been performing long-term studies in this region since 1996 (Linderman et al., 2006; Liu et al., 1999; Viña et al., 2007; Yang et al., 2015) and many findings and methods developed in this study region have been applied to local, regional, national, and international settings (Carter et al., 2014; Li et al., 2013; Liu et al., 2003; Liu and Viña, 2014, Liu et al., 2016).

2.2. Field data

Vegetation surveys were conducted in the summer of 2007 along four trails across the Reserve (numbered 1–4 in Fig. 1). These trails were chosen because they comprise different types of forests and thus provide a good representation of the forest vegetation in the Reserve. The locations of the survey sites were based on a systematic sampling along each trail. To this effect, a starting location was established ca. 100 m from the beginning of each trail (ca. 100 m from the nearest household location in trails 1–3; Fig. 1). Subsequent survey sites were located at regular intervals of 300 steps (i.e., between 200 and 300 m, depending on topography). A total of 62 sites were sampled along the four trails. A 10 m by 20 m rectangular plot was established in each survey site, with its longer axis perpendicular to the trail. The center of each plot was georeferenced using Global Positioning System (GPS) receivers, which were also used to collect elevation data. The overall slope at each plot was determined using a clinometer. Tree stem density was established within each plot by counting all stems with a diameter at breast height larger than 5 cm. The species of each tree counted was recorded, together with the presence of understory bamboo species, when present.

2.3. Remotely sensed data

2.3.1. MODIS data

A time-series of 184 images acquired between January 2005 and December 2008 by the Moderate Resolution Imaging Spectroradiometer (MODIS) onboard NASA's Terra satellite (MOD09A1 – Collection 5; ca. 500 m/pixel) was used to analyze land surface phenology. This image dataset is composed of eight-day composite surface reflectance values collected in seven spectral bands, and corrected for the effects of atmospheric gases, aerosols and thin cirrus clouds (Vermote et al., 1997). This time series of surface reflectance data was used to obtain land surface phenology. Land surface phenology is defined as the seasonal pattern of variation in the vegetated land surface observed using remotely derived vegetation indices. Vegetation indices are mathematical combinations of different spectral bands that constitute semi-analytical measures of vegetation activity. Their main purpose is to enhance the information contained in spectral reflectance data, by extracting the variability due to vegetation characteristics (e.g., leaf area index, vegetation canopy cover) while minimizing soil, atmospheric, and sun-target-sensor geometry effects (Moulin, 1999). Vegetation indices constitute a simple and convenient approach to extract information from remotely sensed data, due to their

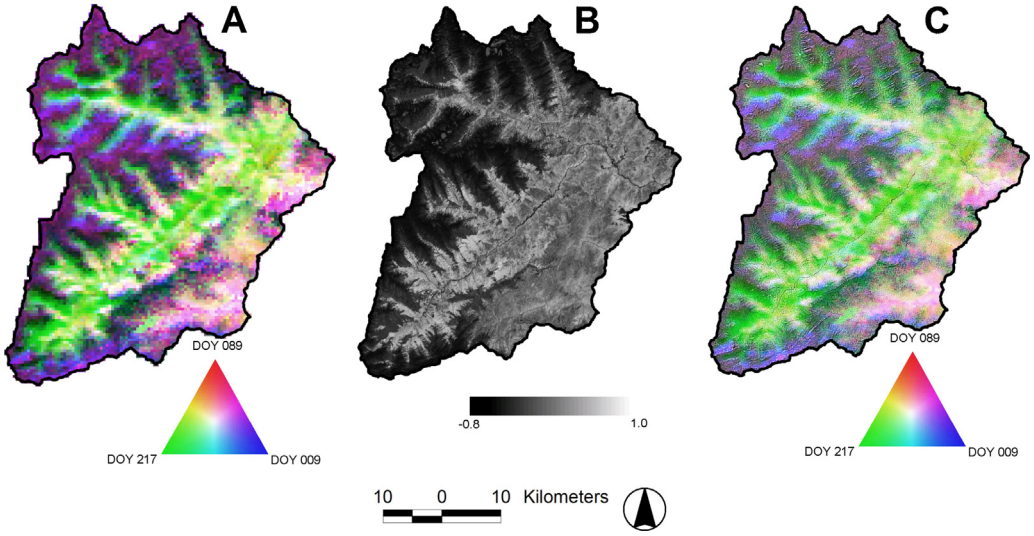

Fig. 2. Spatial distribution of VARI values in the study region (i.e., Wolong Nature Reserve) in (A) three dates of the MODIS time series dataset (i.e., Day of the Year 9, DOY 89 and DOY 217) expressed in the three primary color planes (Red, Green, and Blue, respectively); (B) the Landsat TM/ETM+ datasets (maximum value composite of the Landsat scenes of April 19 and September 18, 2007), and (C) the same three dates as Fig. 2A of the MODIS/Landsat TM/ETM+ fused dataset.

ease of use, which facilitates the processing and analysis of large amounts of data acquired by satellite platforms (Govaerts et al., 1999; Myneni and Hall, 1995). To assess land surface phenology in the study region we used the Visible Atmospherically Resistant Vegetation Index (VARI) (Gitelson et al., 2002) (Fig. 2):

$$\text{VARI} = \frac{\rho_{Green} - \rho_{Red}}{\rho_{Green} + \rho_{Red} - \rho_{Blue}} \quad (1)$$

Where ρ is surface reflectance in the blue, green and red spectral bands of the MODIS sensor system. This index was chosen because it is sensitive not only to changes in chlorophyll content (Gitelson et al., 2002; Perry and Roberts, 2008), but also to changes in the relative content of other foliar pigments such as anthocyanins (Viña and Gitelson, 2011). Therefore, VARI is useful for detecting changes associated with phenophases that go beyond the seasonal variability of photosynthetic biomass (e.g., flowering, fruiting, senescence) (Viña et al., 2004). The phenologic similarity assessed through this index has been successfully related with floristic similarity (Viña et al., 2012), and thus is suitable for assessing changes in floristic similarity across space and through time. VARI has also been used to detect live fuel moisture (Roberts et al., 2006), canopy moisture content (Stow et al., 2005) and water stress (Perry and Roberts, 2008), using different close-range and remote sensors. To minimize the effects of the temporally and spatially extensive cloud cover characteristic of the study region, particularly during the monsoon period (between June and September), we smoothed the time series of VARI by means of an adaptive filter (Savitzky and Golay, 1964) using the Timesat software (Eklundh and Jonsson, 2012). To this effect, a quadratic polynomial function is calculated for all pixels over a moving temporal window, and the observed value is replaced by the value of the polynomial for its respective temporal position in the time series. The result is a smoothed curve adapted to the upper values of the time-series (Eklundh and Jonsson, 2012). The smoothing (i.e., polynomial) function requires data over a moving temporal window, thus, it was necessary to have observational data acquired before and after the targeted temporal window of analysis. In our case, we used data collected in 2005–2008 to obtain a smoothed time series for 2007. Because VARI values under cloudy conditions are lower, this filter is particularly suitable for minimizing the reduction in VARI values due to cloud cover, while retaining the observed seasonal variability of the time series.

2.3.2. Landsat TM/ETM+ data

Cloud-free multi-spectral Landsat 5 Thematic Mapper (TM) and gap-filled Landsat 7 Enhanced Thematic Mapper Plus (ETM+) images (WRS-2 Path 130, Rows 38–39; ca. 30 m/pixel) acquired on April 19, 2007 and September 18, 2007 were obtained geometrically rectified from the United States Geological Survey Global Visualization Viewer (http://glovis.usgs.gov). The level 1T digital number (DN) data of the reflective bands (1 to 5 and 7) of these images were converted to at-sensor radiance and further to at-sensor reflectance following standard procedures (Chander et al., 2009). A linear regression technique was used to match the April 19, 2007 ETM+ images (slaves) to the September 18, 2007 TM images (master). This regression technique was applied separately for each individual band. Per-pixel VARI values were obtained from these radiometrically rectified images and a single VARI value per pixel for the year 2007 was obtained as the maximum value between the two image dates (Fig. 2B).

2.3.3. MODIS/Landsat data fusion

Because of the tradeoffs among spatial, spectral, and temporal resolutions, a sensor system capable of producing images with a fine resolution in all these realms is not currently available. However, as many land change assessments require spatial detail combined with frequent acquisitions, the use of image fusion techniques that blend data from multiple sensor systems for generating synthetic data with finer resolutions is becoming common practice (Boschetti et al., 2015; Gangkofner et al., 2008; Gevaert and García-Haro, 2015; Hilker et al., 2009; Roy et al., 2008). Imagery acquired with a comparatively high spatial resolution such as Landsat TM/ETM+ are commonly used to capture spatial detail, while coarse spatial and high temporal resolution imagery such as MODIS are commonly used to capture fine-temporal changes over time (Hilker et al., 2009). The fusion of these two different datasets therefore theoretically allows capturing fine-temporal changes with a fine spatial detail. Data acquired by the Landsat TM/ETM+ and MODIS sensors are particularly appropriate to be fused given their similar spectral characteristics. In addition, the Landsat 7 (carrying the ETM+ sensor) and the Terra (carrying the MODIS sensor) satellites share the same orbit, thus collect imagery under similar viewing and solar zenith angles, and atmospheric conditions (Roy et al., 2008). The Landsat 5 is also on the same orbit but with an 8-day offset from the Terra acquisition date, thus collects data

under similar viewing and solar zenith angles but with different atmospheric conditions.

For fusing MODIS time series imagery with Landsat TM/ETM+ data, we used the Optimized High-pass Filter Additive (HPFA) technique (Chavez et al., 1991; Schowengerdt, 1980). This technique is a tunable and versatile image fusion method in the spatial domain that allows inserting the structural and textural detail characteristic of datasets with a high spatial resolution into a lower spatial resolution multi-band dataset. In a recent comparison of twelve fusion algorithms, this technique was ranked as one of the best in maintaining high fidelity of spatial and multi-band information (Witharana et al., 2014). The HPFA technique has been optimized, standardized and extended to be applicable to more diverse multi-resolution data sets, while preserving the information content of the original multi-band dataset (Gangkofner et al., 2008). While this technique has been used mainly for obtaining high spatial and spectral imagery, in this study we used it to obtain synthetic imagery with high spatial and temporal resolutions. To this effect, we used the 30 m/pixel image with the maximum VARI value derived from the Landsat TM and ETM+ images for 2007 as the high spatial resolution dataset, and the 500 m/pixel VARI image time series of 2007 (i.e., 46 images) as the low resolution multi-band dataset (Fig. 2C). The maximum VARI value derived from the Landsat TM and ETM+ images of April 19 and September 18, 2007 was used, instead of a single date of imagery (i.e., either the image of April 19 or of September 18), to reduce potential effects of a single phenological stage on the spatial structure of the high spatial resolution dataset.

While currently there are procedures oriented to produce high spatial and temporal multi-spectral fused datasets (Gevaert and García-Haro, 2015; Hilker et al., 2009), such procedures were not required in our analysis given that the entire multi-spectral information of the Landsat TM/ETM+ and MODIS sensors was not needed. Therefore, we chose the HPFA because it is computationally simpler and produces fused image datasets with high fidelity. To test the fidelity of the multi-temporal information contained in the fused high-resolution imagery created with the HPFA technique (Fig. 2C), we regressed the VARI values derived from 200 randomly distributed pixels (with a minimum inter-pixel distance of 600 m) from the synthetic (i.e., MODIS/Landsat fused) image corresponding to the eight-day VARI composite of Day of the Year (DOY) 258–265 in 2007, against those derived from the Landsat TM image of September 19, 2007 (i.e., DOY 262), and found a high significant relationship (Fig. 3). In addition, we used a Mantel test (Legendre, 2000) to assess the divergence between the correlations among the 46 eight-day composite VARI images of the synthetic MODIS/Landsat dataset of 2007 from those of the original MODIS time series imagery of 2007. The Mantel test constitutes a correlation analysis that adjusts for the increased number of cases deriving from the use of correlation matrices (i.e., among the multiple bands of the MODIS and MODIS/Landsat VARI image time series). The significance of this Mantel test was determined through a Monte Carlo permutation analysis in which the rows and columns in the correlation matrices were randomly permuted 999 times. The significance measure corresponds to the number of times the Mantel correlation coefficient of the permuted matrices exceeds the original (i.e., non-permuted) coefficient (Legendre, 2000). A high (i.e., 0.9) and significant ($p < 0.001$) Mantel correlation coefficient was found between the MODIS and the MODIS/Landsat datasets, denoting a high fidelity of the multi-temporal information contained in the fused high-resolution imagery created with the HPFA technique.

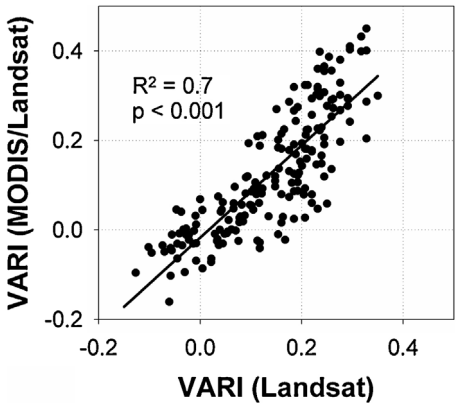

Fig. 3. Relationship between the VARI values derived from 200 randomly distributed pixels (with a minimum inter-pixel distance of 600 m) from the fused (i.e., MODIS/Landsat) image corresponding to the eight-day VARI composite of Day of the Year (DOY) 258–265 in 2007, against those derived from the Landsat TM image of September 19, 2007 (i.e., DOY 262).

2.4. Numerical analyses

2.4.1. Relationship between floristic and phenologic similarities

A matrix of floristic similarity among the 62 field plots was established using the Jaccard index (Jaccard, 1908) for presence–absence of tree and understory bamboo species. To place the field plots in a floristic ordination space, we used this matrix in a non-metric multi-dimensional scaling (NMDS) procedure, which maximizes the rank-order correlation between the similarity measures and the relative distances within the ordination space (Legendre and Legendre, 1998). The relationships among the NMDS ordination axes with topographic variables (i.e., elevation, slope and slope aspect) and distance to the main road (used as an inverse surrogate of human influence) were assessed, while accounting for spatial autocorrelation (Dutilleul, 1993).

To reduce the effects of temporal autocorrelation in the fused MODIS/Landsat VARI image time series, a principal components analysis (PCA) was performed. A few principal components effectively summarize the dominant modes of the spatio-temporal variation, therefore retaining most of the information contained in the image time series (Benedetti et al., 1994; Eklundh and Singh, 1993; Townshend et al., 1985). The first six principal components (explaining ca. 99% of the total variance) were retained.

To assess the relationship between the floristic similarity and the phenologic similarity, we calculated a matrix of inter-pixel (i.e., pixels comprising the 62 field plots) Euclidean distances (converted to similarity by changing their sign) based on the principal components obtained from the fused MODIS/Landsat VARI image time series. This inter-pixel Euclidean distance matrix was correlated with the matrix of inter-plot Jaccard similarities using a Mantel correlation coefficient (Legendre, 2000). The significance of this coefficient was determined through a Monte Carlo permutation analysis in which the rows and columns in the Jaccard similarity or Euclidean distance matrices were randomly permuted 999 times. The significance measure corresponds to the number of times the Mantel correlation coefficient of the permuted matrices exceeded the original (i.e., non-permuted) coefficient (Legendre, 2000). To control for the potential effects of spatial autocorrelation (Borcard et al., 1992), a partial Mantel correlation coefficient (Legendre, 2000) was also calculated using an inter-plot geographic distance matrix as a co-variable.

2.4.2. Use of phenologic similarity as an indicator of floristic similarity

To assess floristic similarity using phenologic similarity, a multiple linear regression model was developed using the floristic ordination axes (i.e., derived from the NMDS) as dependent variables and the phenologic ordination axes (i.e., derived from the

PCA applied to the fused MODIS/Landsat VARI image time series) as independent predictive variables. Model residuals were used to evaluate spatial autocorrelation through the calculation of Moran's I correlograms (Legendre and Legendre, 1998). If spatial autocorrelation of the residuals was significant, spatial autoregressive models (Besag, 1974; Lichstein et al., 2002) were developed to estimate spatially unbiased regression coefficients. Lag and error autoregressive models were computed (Lichstein et al., 2002) and the most appropriate for our datasets was selected, based on the Akaike information criterion (AIC) (Akaike, 1978, 1979).

3. Results

3.1. Patterns of land surface phenology

The average temporal variability of VARI exhibited the typical seasonal pattern of the temperate region (i.e., high and low vegetation index values during seasons with high and low sun angles, respectively) (Fig. 4A). With respect to the spatial (i.e., inter pixel) variability, the VARI exhibited the highest variance in the middle of spring (ca. day of the year 120) and late summer/early autumn (ca. day of the year 240), while the lowest variances occurred in early spring (ca. day of the year 75), summer (ca. day of the year 200) and late autumn (ca. day of the year 300) (Fig. 4A). These distinctive patterns in the timing of highest and lowest inter-pixel variance show the sensitivity of VARI to the phenologic differences among the forests of the study region throughout the year. Such phenologic differences among the forests in the study area are mainly driven by the differences in the timing of leaf green-up and senescence at different elevations. In fact, when related with elevation, the VARI exhibited a bimodal pattern with significant negative correlation coefficients during spring (ca. day of the year 120) and autumn (ca. day of the year 280) (Fig. 4B). This reinforces the strong influence that the elevation gradient has on the patterns of land surface phenology in the forests of the study region.

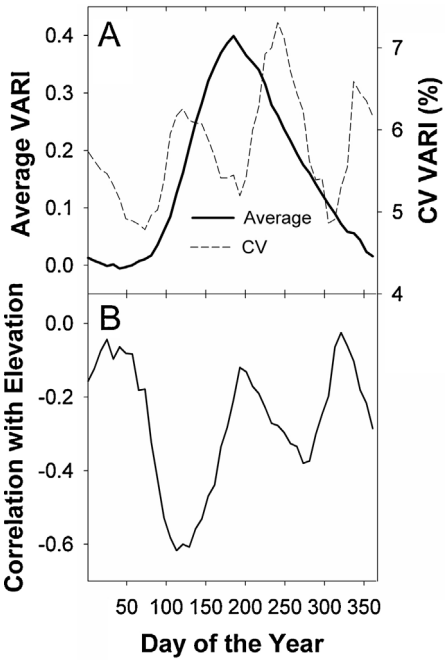

Fig. 4. Temporal profiles of (A) the average and coefficient of variation (CV), and (B) correlation with elevation, of VARI values among the pixels (30 m/pixel) were the 62 field plots were established, obtained from the MODIS/Landsat fused dataset.

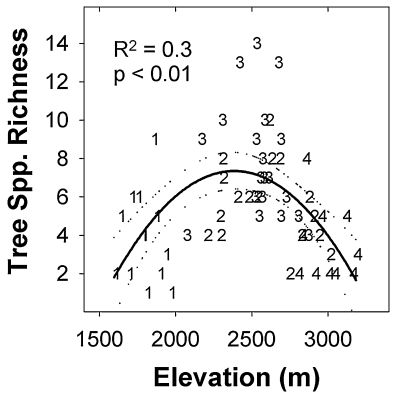

Fig. 5. Relationship between tree species richness and elevation in the 62 field plots established along four transects. Symbol numbers correspond to the four transects along which the field plots were established. The dotted line represents 2 SEM.

3.2. Floristic characteristics

A total of three bamboo species and 68 tree species (see Supplementary Material) were found in the 62 sampling sites distributed along the four transects evaluated. The bamboo species were *Bashania faberi* (Rendle) Yi [=*Arundinaria faberi* Rendle], *Fargesia nitida* (Mitford) Keng f. ex Yi, and *Fargesia robusta* Yi. Dominant tree species (i.e., occurring in ≥20% of the sampling sites) were *Acer laxiflorum* Pax, *Salix dolia* C. K. Schneid, *Prunus pilosiuscula* (C.K. Schneid.) Koehne [=*Cerasus clarofolia* (C.K. Schneid.) T.T. Yu & C.L. Li], *Betula albosinensis*, *Abies faxoniana* Rehder & E.H. Wilson [=*Abies fargesii* var. *faxoniana* (Rehder & E.H. Wilson) Tang S. Liu], *Corylus ferox* Wall. var. *thibetica* (Batalin) Franch. and *Sorbaria arborea* C. K. Schneid.

A significant non-linear relationship was found between species richness and elevation, with the highest richness values being exhibited by sampling sites located at elevations around 2500 m (Fig. 5). This denotes that species richness in the study region is highly influenced by the elevation gradient, with elevations of ca. 2500 m constituting the inflection point of maximum species richness (Fig. 5).

The NMDS procedure, applied to the inter-plot floristic similarity matrix obtained using presence–absence data of tree and bamboo species combined (i.e., using the Jaccard index), generated two orthogonal axes that represent a two-dimensional floristic space (Fig. 6). A significant linear relation (although it became marginally significant, i.e., $p = 0.057$, after accounting for spatial autocorrelation) was found between elevation and axis 1 of the

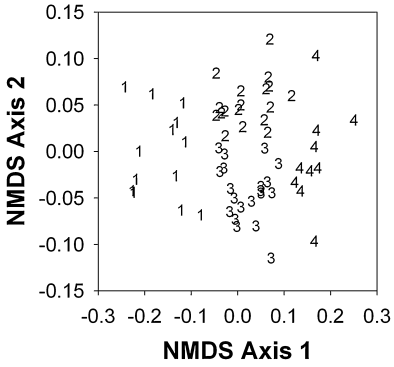

Fig. 6. Two-dimensional ordination space derived from a non-metric multidimensional scaling (NMDS) procedure applied to the floristic similarity among 62 field plots, using the Jaccard index for presence–absence of tree and bamboo species. Symbol numbers correspond to the four transects along which the field plots were established.

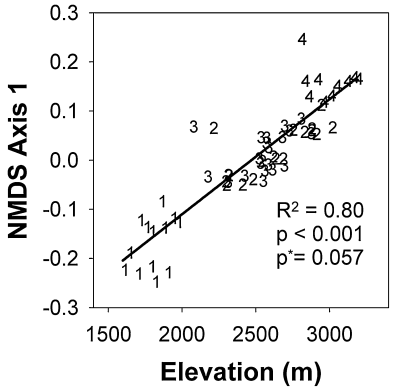

Fig. 7. Relationship between the first axis of the a non-metric multidimensional scaling (NMDS) procedure applied to the floristic similarity among 62 field plots, using the Jaccard index for presence–absence of tree and bamboo species, and elevation. Symbol numbers correspond to the four transects along which the field plots were established. p is the probability of the correlation without accounting for spatial autocorrelation, while p^* is the probability accounting for spatial autocorrelation (Dutilleul, 1993).

NMDS (Fig. 7), which denotes that the elevation gradient is an important variable structuring the species composition in the study region. Without accounting for spatial autocorrelation, axis 2 of the NMDS exhibited a significant relationship with the distance to the main road ($r = 0.406$, $p < 0.01$), which may indicate an effect of human influence on structuring species composition in the study region. However after accounting for spatial autocorrelation this relationship became non-significant ($p = 0.35$).

3.3. Phenologic similarity as an indicator of floristic similarity

A significant Mantel correlation ($r = 0.15$, $p < 0.001$) was found between the similarity in floristic composition (Jaccard index) and the similarity in phenology (Euclidean distance). In addition, the Partial Mantel correlation coefficient obtained using geographic distance as a co-variable to account for potential spatial autocorrelation among field plots, while exhibiting a lower value, was still significant ($r = 0.13$, $p < 0.001$). This denotes a significant relationship between floristic and phenologic similarities, even after accounting for spatial autocorrelation.

Statistically significant linear models relating floristic similarity (i.e., NMDS axes) using phenologic similarity (i.e., principal component axes) were obtained, although they were significantly affected by spatial autocorrelation (Table 1). While both the lag and the error models were significant ($p < 0.001$) for both, the NMDS axis 1 and the NMDS axis 2, the AIC values of the error models were the lowest. Therefore, we present the results of the error models (Table 1). In these spatial autoregressive linear models, the second, third, and fourth principal components were significant predictors of the NMDS axis 1, while the sixth principal component was a significant predictor of the NMDS axis 2 (Table 1). The first principal component was not significant, although it accounts for most of the information in the image time series. However, this component accounts for most of the spatial variability, while it exhibits a lower response to the seasonal variability of the vegetation image time series. The seasonal variability constitutes the most important source of information to assess phenological patterns. These results suggest that phenologic ordination axes obtained using satellite imagery with a high temporal resolution (e.g., MODIS) may be used as suitable predictors of floristic ordination axes obtained using data from field surveys.

Table 1
Coefficients of the spatial auto-regressive error models between the Non-Metric Multidimensional Scaling (NMDS) axes (dependent variables) obtained from the floristic similarity (Jaccard index for presence–absence of tree and bamboo species) matrix among 62 field plots, and the first six principal components (PC) obtained from the MODIS/Landsat TM/ETM+ fused image time series of the Visible Atmospherically Resistant Index (VARI).

Variable	NMDS axis 1	NMDS axis 2
Intercept	0.116824	0.236641
PC1	−0.00133	4.00E−05
PC2	−0.00231†	0.000128
PC3	−0.00577§	−0.00078
PC4	0.003501§	0.000883
PC5	−0.00142	−0.00062
PC6	0.004216	−0.00077*
Spatial autoregressive term	0.613656§	0.547727§
R^2	0.8327	0.4093

* $p < 0.05$.
† $p < 0.01$.
§ $p < 0.001$.

4. Discussion

Results of this study support the hypothesis that there is a significant relationship between floristic similarity and phenologic similarity, and fully agree with the results of a previous study conducted in a different geographic setting (i.e., the Qinling mountains) (Viña et al., 2012). However, a fundamental assumption in the relationship between floristic and phenologic similarity is that the sampled areas in the field correspond with the pixel resolution of the remotely sensed platform used to assess land surface phenology. When using coarse spatial resolution data such as those obtained by the MODIS sensor system, this assumes that the sampled forest stands are homogeneous within each of the MODIS pixels evaluated, an assumption that is seldom realized. Furthermore, given the proximity among field plots in this study, two or more tended to fall within a single MODIS pixel, thus effectively reducing the number of field plots that could be related with the MODIS dataset. Therefore, it is necessary to reconcile the pixel resolution of the sensor system with the sampling areas of the field plots for better utilizing phenologic similarity patterns as indicators of floristic similarity patterns. An optimal solution would be the use of a sensor system with a high resolution in both the spatial and temporal domains. However, such sensor system is not currently available. Thus, it was necessary to explore alternative solutions.

This study showed the suitability of a high spatial and temporal data set produced by the fusion of MODIS and Landsat imagery for assessing the usefulness of phenologic similarity as a surrogate of floristic similarity. This data fusion allowed reconciling the spatial resolutions of field and remotely sensed datasets, and thus proved useful for synoptically analyzing the patterns of floristic similarity using data collected in smaller areas than the footprint of high temporal resolution satellite systems (e.g., MODIS). Nevertheless, it also posed a challenge in which the effects of spatial autocorrelation were pronounced. Therefore, the effects of spatial autocorrelation need to be incorporated into any analysis before using the fusion of high temporal and high spatial resolution remotely sensed datasets for analyzing floristic similarity across space.

The floristic and phenologic patterns observed in the study region are highly influenced by the elevation gradient. On the one hand, a non-linear relationship between species richness and elevation was found. While there are many variables related with elevation that may exert important effects on species richness and composition (e.g., soil characteristics, climate variables), the non-linear pattern observed could be explained by the mid-domain effect, which proposes that a higher number of species tends to occur toward the center of a shared, bounded domain due to geometric boundary constraints in relation to the distribution of

species' range sizes (Colwell et al., 2004). However, given the conspicuous deforestation that occurred in the study region mainly following the elevation gradient (i.e., higher deforestation occurring at elevations below 2500 m while limited or no deforestation close to the tree line) even after the Reserve was established in 1975 (Liu et al., 2001; Viña et al., 2007), the non-linear relation observed could also be explained by the intermediate disturbance hypothesis (Connell, 1978). This is particularly evident by the positive correlation between the NMDS 2 and distance to the main road, which constitutes a surrogate of human influence (thus of human disturbance). However, this correlation was not significant after accounting for spatial autocorrelation, therefore the effects of human disturbance on the floristic composition of the forests in the study area are not completely clear. On the other hand, similar to what has been reported in other regions (Viña et al., 2012), a significant linear relationship between floristic similarity (as measured through the non-metric multidimensional scaling procedure) and elevation was found. This linear relationship suggests that particular species associations tend to occur at different elevations. Furthermore, as was also reported for other regions (Viña et al., 2012), the patterns of land surface phenology were also influenced by the elevation gradient, but following a seasonal pattern in which higher effects are exerted on particular temporal periods (e.g., spring and fall, Fig. 4B). Nevertheless, our analysis was based on the assessment of linear relationships. While such linear approach simplifies the application of the procedure, it does not account for non-linearities and thresholds, which could negatively influence the use of phenologic similarity for assessing floristic similarity. Thus, further studies are needed that incorporate this complexity.

The procedure presented in this article is oriented to assess floristic similarity rather than particular species compositions/associations. Thus, it is general and less constrained by local characteristics, individual species and/or species associations. In addition, it is based not only on spectral variability (as represented by the spatial changes in a vegetation index derived from multiple spectral bands) but also on phenological variability of vegetation canopies. Therefore, it accounts for, and uses the phenological variability of vegetation canopies to assess floristic similarity. However, it is not clear how the relationship between floristic and phenologic similarities will operate in ecosystems exhibiting less pronounced seasonal dynamics, such as tropical rainforests. Thus, it is necessary to assess the applicability of this procedure in such ecosystems, to assess if this procedure will also constitute a valuable tool for mapping and monitoring their floristic diversity patterns.

The use of phenologic similarity, obtained from the fusion of remotely sensed datasets acquired with high spatial and temporal resolutions, as an indicator of floristic similarity has many benefits. On the one hand, it allows assessing the spatial patterns of biodiversity across broad geographic regions and their changes through time. As such, it provides a synoptic and broad geographic view that is seldom provided by the limited spatial extents of traditional and labor-intensive field surveys. On the other hand, it allows to upscale results obtained at local to regional and even continental scales. Therefore, this procedure has many applications in ecology, biogeography and conservation biology. Examples include the capacity to monitor biodiversity patterns across space and over time in response to environmental changes occurring at different spatial scales (e.g., high spatial resolution changes due to land use, low spatial resolution changes due to shifting climate patterns), assessing the spatial congruence among communities or guilds (McKnight et al., 2007) over broad geographic regions, and helping with the identification of areas requiring further conservation actions (e.g., extensions to protected areas, or establishment of new protected areas), among many other applications. All these applications will support a more comprehensive and inclusive conservation of biodiversity (Ferrier, 2002; Xu et al., 2006). We recognize that knowledge on geospatial information analysis and spatial statics are required to successfully implement the procedures described in this study, which may constitute barriers for their adoption by institutions involved in the management of natural resources (e.g., departments of natural resources, nature reserves) especially in the developing world. However, such knowledge is potentially less expensive to acquire than the costs of performing extensive field surveys. Giving the capacity to analyze synoptically the spatial patterns of biodiversity across broad regions, the benefits obtained will outweigh these costs. However, more research is required to make the procedure widely available, for instance through the development of off-the-shelf and open-source software packages.

Acknowledgments

This study was supported by the U.S. National Science Foundation (NSF) [Macrosystems Biology and Dynamics of Coupled Natural and Human Systems (CNH) programs, Office of International Science and Engineering] and Michigan AgBioResearch. The Land Processes Distributed Active Archive Center (LP DAAC), located at the U.S. Geological Survey (USGS) Earth Resources Observation and Science (EROS) Center (lpdaac.usgs.gov) is also acknowledged for the geometrically and radiometrically corrected MODIS and Landsat data sets used in the study. We thank Yahui Zhang, Shumin Fan, Wenbin Yang and Weilin Chen for their help during our field data collection campaign, and Zhiyun Ouyang, Youfu Wang, Fan Yang and Hemin Zhang for their logistic support. Finally, we are grateful to the associate editor Roland Achtziger and two anonymous reviewers for their helpful comments on an earlier version of this paper.

Appendix A. Supplementary data

Supplementary data associated with this article can be found, in the online version, at http://dx.doi.org/10.1016/j.ecolind.2016.01.007.

References

Akaike, H., 1978. Bayesian-analysis of minimum AIC procedure. Ann. Inst. Stat. Math. 30, 9–14.
Akaike, H., 1979. Bayesian extension of the minimum AIC procedure of autoregressive model fitting. Biometrika 66, 237–242.
Asner, G.P., Martin, R.E., 2008. Spectral and chemical analysis of tropical forests: scaling from leaf to canopy levels. Remote Sens. Environ. 112, 3958–3970.
Asner, G.P., Martin, R.E., 2009. Airborne spectranomics: mapping canopy chemical and taxonomic diversity in tropical forests. Front. Ecol. Environ. 7, 269–276.
Benedetti, R., Rossini, P., Taddei, R., 1994. Vegetation classification in the middle Mediterranean area by satellite data. Int. J. Remote Sens. 15, 583–596.
Besag, J., 1974. Spatial interaction and the statistical analysis of lattice systems. J. R. Stat. Soc. B, 192–236.
Borcard, D., Legendre, P., Drapeau, P., 1992. Partialling out the spatial component of ecological variation. Ecology 73, 1045–1055.
Boschetti, L., Roy, D.P., Justice, C.O., Humber, M.L., 2015. MODIS – Landsat fusion for large area 30 m burned area mapping. Remote Sens. Environ. 161, 27–42.
Carlson, K.M., Asner, G.P., Hughes, R.F., Ostertag, R., Martin, R.E., 2007. Hyperspectral remote sensing of canopy biodiversity in Hawaiian lowland rainforests. Ecosystems 10, 536–549.
Carter, N.H., Viña, A., Hull, V., McConnell, W.J., Axinn, W., Ghimire, D., Liu, J., 2014. Coupled human and natural systems approach to wildlife research and conservation. Ecol. Soc. 19, 43.
Chander, G., Markham, B.L., Helder, D.L., 2009. Summary of current radiometric calibration coefficients for Landsat MSS, TM, ETM+, and EO-1 ALI sensors. Remote Sens. Environ. 113, 893–903.
Chavez, P.S., Sides, S.C., Anderson, J.A., 1991. Comparison of 3 different methods to merge multiresolution and multispectral data – Landsat Tm and spot panchromatic. Photogramm. Eng. Remote Sens. 57, 295–303.
Colwell, R.K., Rahbek, C., Gotelli, N.J., 2004. The mid-domain effect and species richness patterns: what have we learned so far? Am. Nat. 163, E1–E23.
Connell, J.H., 1978. Diversity in tropical rain forests and coral reefs. Science 199, 1302–1310.
Dutilleul, P., 1993. Modifying the T-test for assessing the correlation between 2 spatial processes. Biometrics 49, 305–314.

Eklundh, L., Jonsson, P., 2012. TIMESAT 3.2 with Parallel Processing – Software Manual. Lund University.
Eklundh, L., Singh, A., 1993. A comparative-analysis of standardized and unstandardized principal components-analysis in remote-sensing. Int. J. Remote Sens. 14, 1359–1370.
Féret, J.-B., Asner, G.P., 2014. Mapping tropical forest canopy diversity using high-fidelity imaging spectroscopy. Ecol. Appl. 24, 1289–1296.
Ferrier, S., 2002. Mapping spatial pattern in biodiversity for regional conservation planning: where to from here? Syst. Biol. 51, 331–363.
Gangkofner, U.G., Pradhan, P.S., Holcomb, D.W., 2008. Optimizing the high-pass filter addition technique for wage fusion. Photogramm. Eng. Remote Sens. 74, 1107–1118.
Gevaert, C.M., García-Haro, F.J., 2015. A comparison of STARFM and an unmixing-based algorithm for Landsat and MODIS data fusion. Remote Sens. Environ. 156, 34–44.
Gitelson, A.A., Kaufman, Y.J., Stark, R., Rundquist, D., 2002. Novel algorithms for remote estimation of vegetation fraction. Remote Sens. Environ. 80, 76–87.
Govaerts, Y.M., Verstraete, M.M., Pinty, B., Gobron, N., 1999. Designing optimal spectral indices: a feasibility and proof of concept study. Int. J. Remote Sens. 20, 1853–1873.
He, G.M., Chen, X.D., Liu, W., Bearer, S., Zhou, S.Q., Cheng, L.Y.Q., Zhang, H.M., Ouyang, Z.Y., Liu, J.G., 2008. Distribution of economic benefits from ecotourism: a case study of wolong nature reserve for giant pandas in China. Environ. Manage. 42, 1017–1025.
Hilker, T., Wulder, M.A., Coops, N.C., Seitz, N., White, J.C., Gao, F., Masek, J.G., Stenhouse, G., 2009. Generation of dense time series synthetic Landsat data through data blending with MODIS using a spatial and temporal adaptive reflectance fusion model. Remote Sens. Environ. 113, 1988–1999.
Jaccard, P., 1908. Nouvelles recherches sur la distribution florale. Bull. Soc. Vaudoise Sci. Nat. 44, 223–270.
Legendre, P., 2000. Comparison of permutation methods for the partial correlation and partial Mantel tests. J. Stat. Comput. Simul. 67, 37–73.
Legendre, P., Legendre, L., 1998. Numerical Ecology, 2nd English ed. Elsevier Science, The Netherlands.
Li, Y., Viña, A., Yang, W., Chen, X., Zhang, J., Ouyang, Z., Liang, Z., Liu, J., 2013. Effects of conservation policies on forest cover change in giant panda habitat regions, China. Land Use Policy 33, 42–53.
Lichstein, J.W., Simons, T.R., Shriner, S.A., Franzreb, K.E., 2002. Spatial autocorrelation and autoregressive models in ecology. Ecol. Monogr. 72, 445–463.
Lindberg, K., Tisdell, C., Xue, D., 2003. Ecotourism in China's nature reserves. In: Lew, A.A. (Ed.), Tourism in China. Haworth Hospitality Press, New York (pp. xix, 325 p.).
Linderman, M.A., An, L., Bearer, S., He, G., Ouyang, Z., Liu, J., 2006. Interactive effects of natural and human disturbances on vegetation dynamics across landscapes. Ecol. Appl. 16, 452–463.
Liu, J., Daily, G.C., Ehrlich, P.R., Luck, G.W., 2003. Effects of household dynamics on resource consumption and biodiversity. Nature 421, 530–533.
Liu, J., Linderman, M., Ouyang, Z., An, L., Zhang, H., 2001. Ecological degradation in protected areas: the case of Wolong Nature Reserve for giant pandas. Science 292, 98.
Liu, J., Ouyang, Z., Taylor, W., Groop, R., Tan, Y., Zhang, H., 1999. A framework for evaluating effects of human factors on wildlife habitats: the case on the giant pandas. Conserv. Biol. 13, 1360–1370.
Liu, J., Viña, A., 2014. Pandas, plants and people. Ann. Mo. Bot. Gard. 100, 108–125.
Liu, J., Hull, V., Yang, W., Viña, A., Chen, X., Ouyang, Z., Zhang, H. (Eds.), 2016. Pandas and People - Coupling Human and Natural Systems for Sustainability. Oxford University Press, p. 299.
McKnight, M.W., White, P.S., McDonald, R.I., Lamoreux, J.F., Sechrest, W., Ridgely, R.S., Stuart, S.N., 2007. Putting beta-diversity on the map: broad-scale congruence and coincidence in the extremes. PLoS Biol. 5, 2424–2432.
Moulin, S., 1999. Impacts of model parameter uncertainties on crop reflectance estimates: a regional case study on wheat. Int. J. Remote Sens. 20, 213–218.
Myers, N., Mittermeier, R.A., Mittermeier, C.G., da Fonseca, G.A.B., Kent, J., 2000. Biodiversity hotspots for conservation priorities. Nature 403, 853–858.
Myneni, R.B., Hall, F.G., 1995. The interpretation of spectral vegetation indexes. IEEE Trans. Geosci. Remote Sens. 33, 481–486.
Perry, E.M., Roberts, D.A., 2008. Sensitivity of narrow-band and broad-band indices for assessing nitrogen availability and water stress in an annual crop. Agron. J. 100, 1211–1219.
Reid, D.G., Hu, J., 1991. Giant panda selection between *Bashania fangiana* bamboo habitats in Wolong Reserve, Sichuan, China. J. Appl. Ecol. 28, 228–243.
Roberts, D.A., Dennison, P.E., Peterson, S., Sweeney, S., Rechel, J., 2006. Evaluation of airborne visible/infrared imaging spectrometer (AVIRIS) and moderate resolution imaging spectrometer (MODIS) measures of live fuel moisture and fuel condition in a shrubland ecosystem in southern California. J. Geophys. Res.-Biogeosci. 111, G01S02.
Rocchini, D., 2007. Distance decay in spectral space in analysing ecosystem beta-diversity. Int. J. Remote Sens. 28, 2635–2644.
Rocchini, D., Balkenhol, N., Carter, G.A., Foody, G.M., Gillespie, T.W., He, K.S., Kark, S., Levin, N., Lucas, K., Luoto, M., Nagendra, H., Oldeland, J., Ricotta, C., Southworth, J., Neteler, M., 2010. Remotely sensed spectral heterogeneity as a proxy of species diversity: recent advances and open challenges. Ecol. Inf. 5, 318–329.
Rose, R.A., Byler, D., Eastman, J.R., Fleishman, E., Geller, G., Goetz, S., Guild, L., Hamilton, H., Hansen, M., Headley, R., 2015. Ten ways remote sensing can contribute to conservation. Conserv. Biol. 29, 350–359.
Roy, D.P., Ju, J., Lewis, P., Schaaf, C., Gao, F., Hansen, M., Lindquist, E., 2008. Multi-temporal MODIS-Landsat data fusion for relative radiometric normalization, gap filling, and prediction of Landsat data. Remote Sens. Environ. 112, 3112–3130.
Savitzky, A., Golay, M.J.E., 1964. Smoothing and differentiation of data by simplified least squares procedures. Anal. Chem. 36, 1627–1639.
Schaller, G.B., Hu, J., Pan, W., Zhu, J., 1985. The Giant Pandas of Wolong. University of Chicago Press, Chicago.
Schowengerdt, R.A., 1980. Reconstruction of multispatial, multispectral image data using spatial-frequency content. Photogramm. Eng. Remote Sens. 46, 1325–1334.
State Forestry Administration, 2006. The 3rd National Survey Report on Giant Panda in China. Science Publisher, Beijing, China (in Chinese).
Stow, D., Niphadkar, M., Kaiser, J., 2005. MODIS-derived visible atmospherically resistant index for monitoring chaparral moisture content. Int. J. Remote Sens. 26, 3867–3873.
Taylor, A.H., Qin, Z.S., 1993. Bamboo regeneration after flowering in the Wolong Giant Panda Reserve, China. Biol. Conserv. 63, 231–234.
Thessler, S., Ruokolainen, K., Tuomisto, H., Tomppo, E., 2005. Mapping gradual landscape-scale floristic changes in Amazonian primary rain forests by combining ordination and remote sensing. Global Ecol. Biogeogr. 14, 315–325.
Townshend, J.R.G., Goff, T.E., Tucker, C.J., 1985. Multitemporal dimensionality of images of normalized difference vegetation index at continental scales. IEEE Trans. Geosci. Remote Sens. 23, 888–895.
Tuanmu, M.-N., Viña, A., Bearer, S., Xu, W., Ouyang, Z., Zhang, H., Liu, J., 2010. Mapping understory vegetation using phenological characteristics derived from remotely sensed data. Remote Sens. Environ. 114, 1833–1844.
Tuanmu, M.N., Viña, A., Roloff, G.J., Liu, W., Ouyang, Z.Y., Zhang, H.M., Liu, J.G., 2011. Temporal transferability of wildlife habitat models: implications for habitat monitoring. J. Biogeogr. 38, 1510–1523.
Tuomisto, H., Poulsen, A.D., Ruokolainen, K., Moran, R.C., Quintana, C., Celi, J., Canas, G., 2003. Linking floristic patterns with soil heterogeneity and satellite imagery in Ecuadorian Amazonia. Ecol. Appl. 13, 352–371.
Turner, W., 2014. Sensing biodiversity. Science 346, 301–302.
Turner, W., Spector, S., Gardiner, N., Fladeland, M., Sterling, E., Steininger, M., 2003. Remote sensing for biodiversity science and conservation. Trends Ecol. Evol. 18, 306–314.
Vermote, E.F., ElSaleous, N., Justice, C.O., Kaufman, Y.J., Privette, J.L., Remer, L., Roger, J.C., Tanre, D., 1997. Atmospheric correction of visible to middle-infrared EOS-MODIS data over land surfaces: background, operational algorithm and validation. J. Geophys. Res.-Atmos. 102, 17131–17141.
Viña, A., Bearer, S., Chen, X., He, G., Linderman, M., An, L., Zhang, H., Ouyang, Z., Liu, J., 2007. Temporal changes in giant panda habitat connectivity across boundaries of Wolong Nature Reserve, China. Ecol. Appl. 17, 1019–1030.
Viña, A., Bearer, S., Zhang, H., Ouyang, Z., Liu, J., 2008. Evaluating MODIS data for mapping wildlife habitat distribution. Remote Sens. Environ. 112, 2160–2169.
Viña, A., Chen, X.D., McConnell, W.J., Liu, W., Xu, W.H., Ouyang, Z.Y., Zhang, H.M., Liu, J., 2011. Effects of natural disasters on conservation policies: the case of the 2008 Wenchuan Earthquake, China. Ambio 40, 274–284.
Viña, A., Gitelson, A.A., 2011. Sensitivity to foliar anthocyanin content of vegetation indices using green reflectance. IEEE Geosci. Remote Sens. Lett. 8, 464–468.
Viña, A., Gitelson, A.A., Rundquist, D.C., Keydan, G., Leavitt, B., Schepers, J., 2004. Monitoring maize (*Zea mays* L.) phenology with remote sensing. Agron. J. 96, 1139–1147.
Viña, A., Tuanmu, M.-N., Xu, W., Li, Y., Ouyang, Z., DeFries, R., Liu, J., 2010. Range-wide analysis of wildlife habitat: implications for conservation. Biol. Conserv. 143, 1960–1969.
Viña, A., Tuanmu, M.-N., Xu, W., Li, Y., Qi, J., Ouyang, Z., Liu, J., 2012. Relationship between floristic similarity and vegetated land surface phenology: implications for the synoptic monitoring of species diversity at broad geographic regions. Remote Sens. Environ. 121, 488–496.
Witharana, C., Civco, D.L., Meyer, T.H., 2014. Evaluation of data fusion and image segmentation in earth observation based rapid mapping workflows. ISPRS J. Photogram. Rem. Sens. 87, 1–18.
Xu, W.H., Ouyang, Z., Viña, A., Zheng, H., Liu, J.G., Xiao, Y., 2006. Designing a conservation plan for protecting the habitat for giant pandas in the Qionglai mountain range, China. Divers. Distrib. 12, 610–619.
Yang, W., Dietz, T., Kramer, D.B., Ouyang, Z., Liu, J., 2015. An integrated approach to understanding the linkages between ecosystem services and human well-being. Ecosyst. Health Sustain. 1, art19.